Accelerated Reduced Gradient Algorithm with Constraint Relaxation in Differential Inverse Kinematics

Bence Varga
Doctoral School of Applied Informatics and Applied Mathematics
Bánki Donát Faculty of Mechanical and Safety Engineering
Óbuda University
Budapest, Hungary
varga.bence@bgk.uni-obuda.hu

Hazem Issa
Doctoral School of Applied Informatics and Applied Mathematics
Óbuda University
Budapest, Hungary
hazem.issa@uni-obuda.hu

Richárd Horváth
Bánki Donát Faculty of Mechanical and Safety Engineering
Óbuda University
Budapest, Hungary
ORCID: 0000-0002-4924-3244

József K. Tar
Doctoral School of Applied Informatics and Applied Mathematics
John von Neumann Faculty of Informatics
Antal Bejczy Center of Intelligent Robotics
Óbuda University
Budapest, Hungary
ORCID: 0000-0002-5476-401X

***Abstract*—The Moore-Penrose pseudoinverse-based solution of the differential inverse kinematic task of redundant robots corresponds to the result of a particular optimization under constraints in which the implementation of Lagrange's Reduced Gradient Algorithm can be evaded simply by considering the zero partial derivatives of the "Auxiliary Function" associated with this problem. This possibility arises because of the fact that the cost term is built up of quadratic functions of the variable of optimization while the constraint term is linear function of the same variables. Any modification in the cost and/or constraint structure makes it necessary the use of the numerical algorithm. Anyway, the penalty effect of the cost terms is always overridden by the hard constraints that makes practical problems in the vicinity of kinematic singularities where the possible solution still exists but needs huge joint coordinate time-derivatives. While in the special case the pseudoinverse simply can be deformed, in the more general one more sophisticated constraint relaxation can be applied. In this paper a formerly proposed accelerated treatment of the constraint terms is further developed by the introduction of a simple constraint relaxation. Furthermore, the numerical results of the algorithm are smoothed by a third order tracking strategy to obtain dynamically implementable solution. The improved method's operation is exemplified by computation results for a 7 degree of freedom open kinematic chain.**

***Index Terms*—differential inverse kinematic task; reduced gradient algorithm; Moore-Penrose pseudoinverse; redundant open kinematic chain; constraint relaxation.**

This research was supported by the Doctoral School of Applied Informatics and Applied Mathematics of Óbuda University.

I. Introduction

As is well known the inverse kinematic task of open kinematic chain has closed form analytical solutions only for special constructions as e.g., the 6 degree of freedom PUMA type arm (e.g., [1]–[3]). Such a solution normally is possible only if three orthogonal axles have a single common intersection point. To obtain more dexterous robot arms often redundant constructions are used that were widely investigated in the past (e.g., [4]–[7]). To select a particular solution of the pool of the infinitely many ones normally the Moore-Penrose pseudoinverse [8]–[10] is used because it minimizes the sum of the squares of the joint coordinate time-derivatives that can be interpreted as the most economical one that is exempt of the unnecessary motion of the joints. This "basic solution" later can be "colored" by adding to it certain elements of the null space of the Jacobian of the problem to take into consideration additional complementary points of view.

From mathematical point of view the background behind the Moore-Penrose pseudoinverse is the more general task called "optimization under constraints" that normally numerically can be solved by using Lagrange's "Reduced Gradient Algorithm". Though Lagrange suggested this method for developing Analytical Classical Mechanics [11], the appearance of modern computers made it possible to implement it as a general numerical solver to tackle various practical problems under the name "Nonlinear Programming" (e.g., [12]–[17]). In many cases the Lagrange multipliers that are used in the

Cite as: B. Varga, H. Issa, R. Horváth, and J. Tar, "Accelerated Reduced Gradient Algorithm with Constraint Relaxation in Differential Inverse Kinematics", *Syst. Theor. Control Comput. J.,* vol. 1, no. 2, pp. 21–32, Dec. 2021.
DOI: 10.52846/stccj.2021.1.2.23

gradient reduction process have clear physical meaning (e.g., [18]) that, for instance in chemistry leads to the application of the Legendre transformation and the introduction of chemical potentials [19], in Classical Mechanics to Hamilton's canonical equations of motion [20], [21] and to the use of the "co-state variable" in optimal control in similar manner as the canonical momentum is associated with the canonical coordinates in Hamiltonian Classical Mechanics (e.g., [22]–[24]). On this basis an analogy can be observed between the solution and the flow of incompressible fluids from which expectations for the convergence properties of this approach generally can be concluded.

It is generally true that where Lagrange's algorithm stops the partial derivative of the "Auxiliary Function" according to its each variable is zero. In the case of the Moore-Penrose pseudoinverse this information immediately can be used for obtaining the solution in the form of (1)

$$\dot{q}_i = J^T(q) \left[J(q) J^T(q) \right]^{-1} \dot{x} \ , \tag{1}$$

where q_i denotes the i^{th} joint coordinate and $\dot{x}$ contains the Cartesian workshop-based coordinates of the Tool Center Point (TCP) of the robot arm, and further 3 other components that describe the "pose" of the gripped workpiece. The matrix $J(q)$ denotes the Jacobian of the problem. Where the quadratic matrix $J(q)J^T(q)$ cannot be inverted the kinematic chain is singular. To avoid the occurrence of infinite joint coordinate time-derivatives, in solving a similar problem, Levenberg and Marquardt suggested a little distortion of this matrix [25], [26] as

$$\dot{q}_i = J^T(q) \left[J(q) J^T(q) + \mu I \right]^{-1} \dot{x} \ , \tag{2}$$

in which I is the identity matrix, and $0 < \mu$ is a small number in comparison with the smallest nonzero eigenvalue of $J(q)J^T(q)$. The matrix in (2) is always invertible, and in the non-singular points causes only minimal modification of the solution.

In [27] a novel approach was outlined for solving the inverse kinematic task of redundant open kinematic chains of general structure in which the main point was the introduction of more sophisticated cost function than that of the Moore-Penrose pseudoinverse. As a consequence the need for using the numerical algorithm naturally arose together with the question whether is it really necessary to introduce the co-state variables? The generalization of the Moore-Penrose pseudoinverse for non-quadratic cost function with co-state variables can be formulated as follows:

$$\text{minimize} \sum_i \Psi(q_i, \dot{q}_i) \text{ under the constraints} \tag{3a}$$

$$g_s(q, \dot{q}) \equiv \sum_j J_{sj}(q) \dot{q}_j - \dot{x}_s = 0 \, \forall s \ , \tag{3b}$$

in which the variables of the optimization are the time-derivatives $\dot{q}_s$, however, Ψ, and consequently $\frac{\partial \Psi}{\partial \dot{q}_s}$ also may depend on the coordinates q. In this case the reduced gradient in Lagrange's algorithm would be

$$\Phi_i \equiv \frac{\partial \Psi(q_i, \dot{q}_i)}{\partial \dot{q}_i} + \sum_s \lambda_s \frac{\partial g_s(q, \dot{q})}{\partial \dot{q}_i} \ , \tag{4}$$

and each Lagrange multiplier should be individually computed by solving the linear equation obtained from the requirement that each *constraint gradient* $\frac{\partial g_s}{\partial \dot{q}}$ must be orthogonal to Φ. Since orthogonality means zero scalar product, the linear equation to be solved for $\{ \lambda_s \}$ would be

$$\left\langle \frac{\partial g_u(q, \dot{q})}{\partial \dot{q}}, \frac{\partial \sum_i \Psi(q_i, \dot{q}_i)}{\partial \dot{q}} + \sum_s \lambda_s \frac{\partial g_s(q, \dot{q})}{\partial \dot{q}} \right\rangle = 0 \ , \tag{5}$$

and the matrix of elements

$$M_{us} \equiv \left(\frac{\partial g_u(q, \dot{q})}{\partial \dot{q}} \right)^T \left(\frac{\partial g_s(q, \dot{q})}{\partial \dot{q}} \right) \tag{6}$$

should be inverted. In [27] it was realized that the computational burden of this matrix inversion can be avoided if the fact that $\forall s \, g_s(q, \dot{q}) = 0$ holds if and only if $G(q, \dot{q}) \equiv \sum_s g_s^2(q, \dot{q}) = 0$ is taken into consideration. In this case the optimization problem (7)

$$\text{minimize} \sum_i \Psi(q_i, \dot{q}_i) \text{ under the constraint} \tag{7a}$$

$$G(q, \dot{q}) \equiv \sum_s \left(\sum_j J_{sj}(q) \dot{q}_j - \dot{x}_s \right)^2 = 0 \tag{7b}$$

should be solved instead of the original one in (3), and only the introduction of a single Lagrange multiplier is necessary in the reduced gradient in (8) as

$$\Phi_i \equiv \frac{\partial \Psi(q_i, \dot{q}_i)}{\partial \dot{q}_i} + \lambda \frac{\partial G(q, \dot{q})}{\partial \dot{q}_i} \tag{8}$$

instead of the numerous multipliers in the original problem in (4). In this manner the inversion of the matrix in (6) can be evaded and the algorithm can be accelerated.

In [27] numerical calculations were done for very complicated $\Psi(q_i, \dot{q}_i)$ terms and the problem that in the vicinity of the singularities the *"hard constraint"* $G(q, \dot{q}) = 0$ overrides the *"penalizing effect"* of the cost function was well pointed out. In [28] a special approach applying the formalism of the Receding Horizon Controllers [29] was suggested to relax this hard constraint. In the present approach an alternative "constraint softening" method is presented.

II. A Simple Method for Softening the Constraint Terms

In control technology in the subject area of H_∞ filtering problems *typical cost functions* occur the positive nature of which cannot be taken for granted, in the form of $\|z - \hat{z}\|_2^2 - \gamma^2 \left[\|w\|_2^2 + \|v\|_2^2 \right]$ (e.g., [30]), in which the positive constant γ must be cautiously set to maintain convergence. The qualitative interpretation of this expression is evident: the first term can be regarded as the norm of some "error" with the absolute minimum of 0. The second term means the addition of certain

negative contributions, therefore the absolute minimum of the sum (if it exists, depending on γ) may occur at points in which the first term is positive. In this manner the occurrence of greater errors can be allowed in the first term.

Evidently, a similar idea can be applied *in the constraint term* of the optimization problem in (7) where $G(q,\dot{q}) \geq 0$ and achieving the absolute minimum (i.e., obtaining the exact solution of the inverse kinematic task) is desirable only if the $|\dot{q}_i|$ values are not *"impractically big"*. Therefore, for "small" $|\dot{q}_i|$ values no softening is necessary. However, if in the exact solution certain $|\dot{q}_i|$ values are greater than some practical limit, the addition of certain negative contribution to $G(q,\dot{q})$ is desirable in the form of (9)

$$\tilde{G}(q,\dot{q}) = G(q,\dot{q}) + \sum_i Z(\dot{q}_i) \tag{9}$$

in which

$$Z(\dot{q}_i) = \begin{cases} 0 \text{ if } |\dot{q}_i| \leq w_S \ , \\ \dfrac{-h_S(\dot{q}_i - w_S)}{w_S} \text{ if } w_S < \dot{q}_i \leq 2w_S \ , \\ -h_S \text{ if } 2w_S < \dot{q}_i \ , \\ -h_S + \dfrac{h_S(\dot{q}_i + 2w_S)}{w_S} \text{ if} \\ -2w_S < \dot{q}_i < -w_S \ , \\ -h_S \text{ if } \dot{q}_i < -2w_S \ . \end{cases} \tag{10}$$

In the simulations presented in (10) the numerical values of $w_S = 4.0\,\mathrm{rad/s}$ and $h_S = 100.0$ were chosen, the graph of the function is shown in Fig. 1.

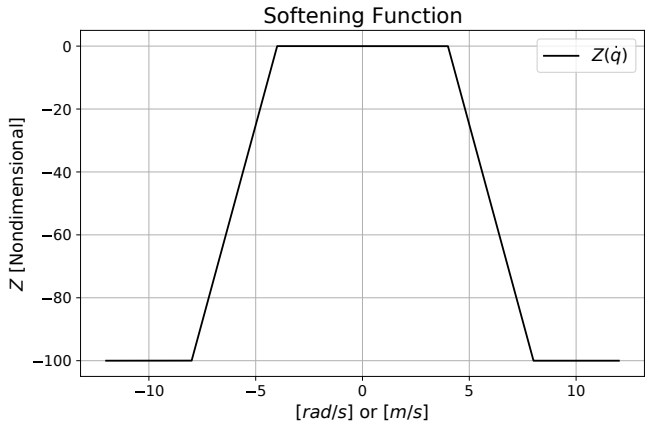

Fig. 1. The constraint softening function applied in the simulations.

It is important to note that in this case the negative contributions have a common lower bound, consequently the optimization algorithm can remain convergent for small enough w_S and h_S: the trajectory can be tracked with limited precision. (Of course, divergence may happen, i.e., the trajectory to be tracked "can be lost" but this situation can be evaded by decreasing these parameters.) Even if one of the $|\dot{q}_i|$ values is too big, the $\tilde{G} = 0$ constraint allows $G > 0$, i.e., the original task will be relaxed and this relaxation can be "distributed" between the members of the set $\{\dot{q}_i\}$. It is worth nothing that the approximate numerical differentiation of the function in Fig. 1 does not mean practical problem. In the sequel simulation investigations will be presented.

III. Simulation Results

To better reveal the near singular configurations, in contrast to the special structure that was considered in [27] (it contained one prismatic axle in a 7 degree of freedom structure), in the present paper each axle was rotational. Its details are given in the sequel.

A. The Kinematic Structure Investigated

The *"Home Position"* of the kinematic structure is given in Fig. 2. As in [27], the Inverse Kinematic Task of a robot can be described by the desired position of the *"Tool Center Point (TCP)"* r with respect to the Cartesian "Workshop Coordinates of Reference", and the desired pose O of the workpiece or the tool that can be achieved by various joint coordinates $q_1, q_2, \cdots, q_n$ (it is an ambiguous solution).

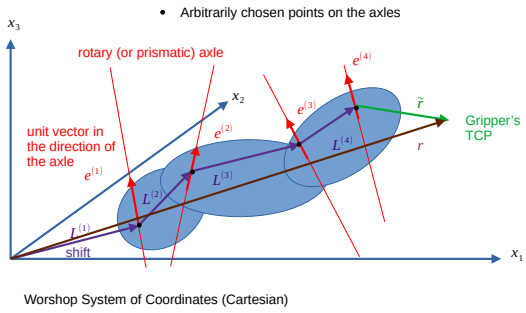

Fig. 2. The "Home Position" of the kinematic structure.

The velocity of the TCP is given by (11)

$$\begin{bmatrix} \dot{r}(t) \\ 0 \end{bmatrix} = \Big(\dot{q}_1 \frac{\mathrm{d}H^{(1)}}{\mathrm{d}q_1} H^{(1)^{-1}} + \dot{q}_2 H^{(1)} \frac{\mathrm{d}H^{(2)}}{\mathrm{d}q_2} H^{(2)^{-1}} H^{(1)^{-1}} + \ldots + \\ + \dot{q}_n H^{(1)} H^{(2)} \cdots \\ \cdots H^{(n-1)} \frac{\mathrm{d}H^{(n)}}{\mathrm{d}q_n} H^{(n)^{-1}} H^{(n-1)^{-1}} \\ \cdots H^{(2)^{-1}} H^{(1)^{-1}} \Big) \begin{bmatrix} r(t) \\ 1 \end{bmatrix} , \tag{11}$$

in which each axle was rotary, i.e., the homogeneous matrices in (11) were defined as

$$H^{(i)}\left(q_i, e^{(i)}, L^{(i)}\right) \equiv \begin{bmatrix} O\left(q_i, e^{(i)}\right) & L^{(i)} \\ 0^T & 1 \end{bmatrix} \tag{12}$$

in which the components of the unit vector e are distributed in the generator of the rotation $\mathcal{G} = \begin{bmatrix} 0 & -e_3 & e_2 \\ e_3 & 0 & -e_1 \\ e_2 & e_1 & 0 \end{bmatrix}$, and the appropriate rotational matrix is computed by the Rodrigues

formula [31] as $O^{(i)} = I + \sin q_i \mathcal{G}^{(i)} + (1 - \cos q_i)\mathcal{G}^{(i)^2}$. In the matrix in (11) the upper left block of size 3×3 determines the skew symmetric rotational velocity of the object gripped by the robot. In this equation the element of a linear space, the tangent space of the group of the homogeneous matrices at the identity matrix, that describes the motion of the workpiece $G(t)$, is expressed as a linear combination of the vectors of this linear space $\left\{G^{(i)}(q(t))\right\}$ expressed by the joint coordinate velocities $\dot{q}_i$ in (13).

$$\sum_{i=1}^{n} \dot{q}_i G^{(i)}(q(t)) = G(t) \ . \tag{13}$$

For getting rid of unnecessary redundancies the independent components can be placed in the Jacobian of the problem. Since the upper left block of $G^{(i)}$ is always skew-symmetric, and the 4^{th} row is always zero, the independent elements of $G^{(i)}(q(t))$ and that of $G(t)$ can be placed into a column containing 6 rows as:

$$G^{(i)} \Leftrightarrow \mathbf{R}^6 \ni J^{(i)} = \begin{bmatrix} G^{(i)}_{12} \\ G^{(i)}_{13} \\ G^{(i)}_{23} \\ G^{(i)}_{14} \\ G^{(i)}_{24} \\ G^{(i)}_{34} \end{bmatrix} \ , \tag{14}$$

$$G \Leftrightarrow \mathbf{R}^6 \ni \dot{x} = \begin{bmatrix} G_{12} \\ G_{13} \\ G_{23} \\ G_{14} \\ G_{24} \\ G_{34} \end{bmatrix} \ , \mathbf{R}^n \ni \dot{\xi} = \begin{bmatrix} \dot{q}_1 \\ \vdots \\ \dot{q}_n \end{bmatrix} \ .$$

In our case for $n = 7$ the following *kinematic parameters* were applied (using the syntax of Julia language [32]): the unit vectors and the shift parameters of the homogeneous matrices were placed into the columns of matrices as

```
r_tilde=[1.0;0.0;0.0;1.0] # for the TCP

# The unit vectors of axles
es=[0 0 0 1 1 0 0;
    0 1 1 0 0 1 0;
    1 0 0 0 0 0 1] # nondimensional

# The shift parameters
h_=1.0
S_=2.0
l_=1.0
L_=0.5

rs=[0  0  S_ l_ L_ 0 0;
    0  0  0  0  0  0 0;5
    h_ 0  0  l_ 0  0 0] # [m]
```

B. The Cost Functions

In contrast to the very complex structure used in [27], in the present paper the simpler choice was investigated as

$$\Psi(q, \dot{q}) = \sum_{i=1}^{7} C_i \left[\frac{\dot{q}_i}{\Delta_{\dot{q}_i}}\right]^4 \left|\frac{q_i}{\Delta_{q_i}}\right|^{P_i} \ . \tag{15}$$

Though the gradient is produced only according tho the variable $\dot{q}$, the value of the contribution in the penalty and its gradient also depend on q: high joint velocities $\dot{q}_i$ are better penalized if $|q_i|$ is too big. By using te power 4 for $\dot{q}_i$ the way of penalization is seriously different to that of quadratic penalty functions. In the computations for each i $\Delta_{q_i} = 0.8$, $P_i = 2$, $\Delta_{\dot{q}_i} = 0.5 w_S$, and $C_i \in [1, 6, 1, 8, 2, 8, 1]$ were chosen.

Because the reduced gradient algorithm is numerically stropped at a limit value associated with the norm of the reduced gradient (in the computations the steps $-\alpha_2 \Phi_i$ were done in (8) with $\alpha_2 = 10^{-5}$, and the algorithm was stopped when the condition $\|\Phi\| \leq 10^{-4}$ was met), in the case of a fine time-resolution the numerically computed values somehow must be smoothed to obtain a dynamically traceable trajectory for the robot. Similarly to the method also used by Bodó et Lantos in [33] for a positive constant parameter Λ_S the noisy function $u(t)$ can be tracked by a smoothed function $f(t)$ in the following manner:

$$\left(\frac{\mathrm{d}}{\mathrm{d}t} + \Lambda_S\right)^3 f(t) = \Lambda_S^3 u(t) \tag{16}$$

that in the frequency domain (by the use of the Laplace transform) has the transmission function

$$F(s) = \frac{\Lambda_S^3 U(s)}{s^3 + 3s^2\Lambda_S + 3s\Lambda_S^2 + \Lambda_S^3} \ , \tag{17}$$

that for zero frequency $s = 0$ (i.e., constant signal) yields the value 1, and for high frequencies quickly converges to 0. Therefore, it can precisely track "slow signals" (this concept numerically is "defined" by the actual value of Λ_S), and rejects the higher frequency terms that are caused by the numerical fluctuations in $u(t)$. (In [27] no such filtering was applied.) In the computations $\Lambda_S = 200.0\, s^{-1}$ was used.

C. Numerical Results

In the simulations results obtained without and with smoothing, and without constraint relaxation (in this case $h_S = 0$ was chosen) and with constraint relaxation (with $h_S = 100.0$) are shown and compared with each other.

Figs. 3, 4, 5, and 6 reveal: the constraint relaxation made it visible that the trajectory had three near singularity sections. The tracking precision was to some extent corrupted by the smoothing algorithm (Figs. 7, 8, 9, 10 11, 12, 13, and 14).

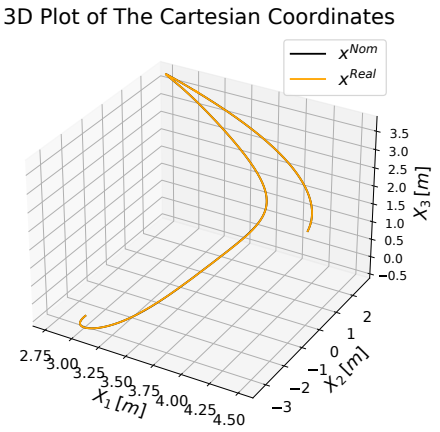

Fig. 3. The 3D Cartesian figure of the trajectory of the TCP without constraint relaxation, without smoothing.

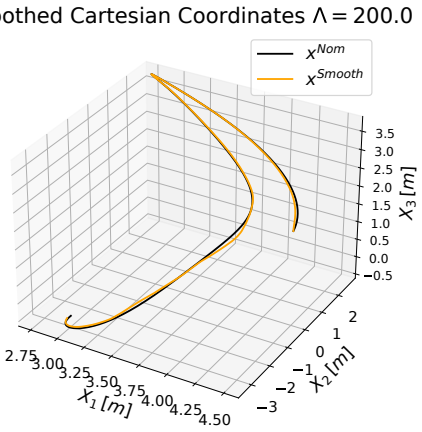

Fig. 6. The 3D Cartesian figure of the trajectory of the TCP with constraint relaxation, with smoothing).

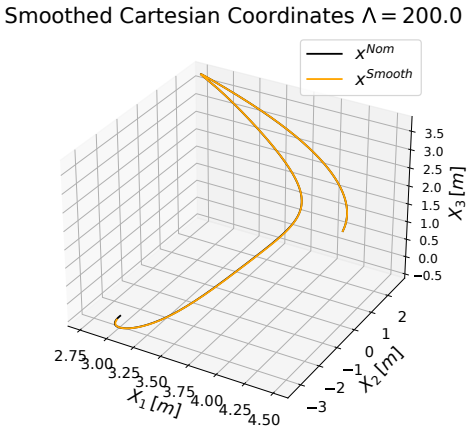

Fig. 4. The 3D Cartesian figure of the trajectory of the TCP without constraint relaxation, with smoothing).

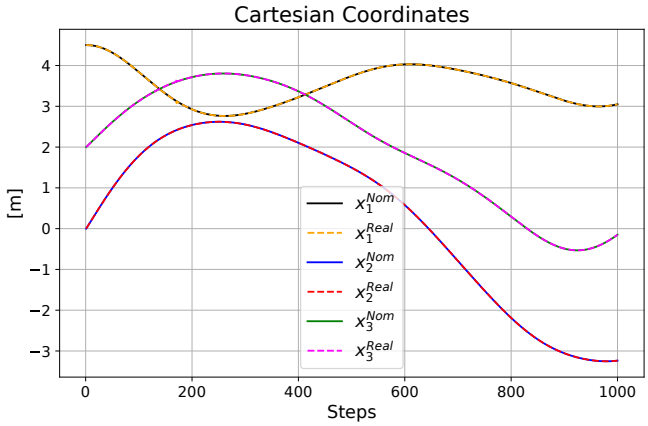

Fig. 7. The Cartesian coordinates of the trajectory of the TCP without constraint relaxation, without smoothing.

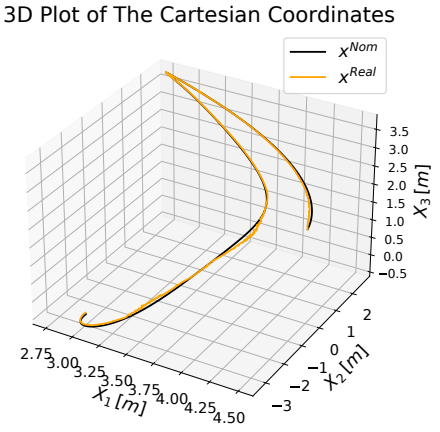

Fig. 5. The 3D Cartesian figure of the trajectory of the TCP with constraint relaxation, without smoothing.

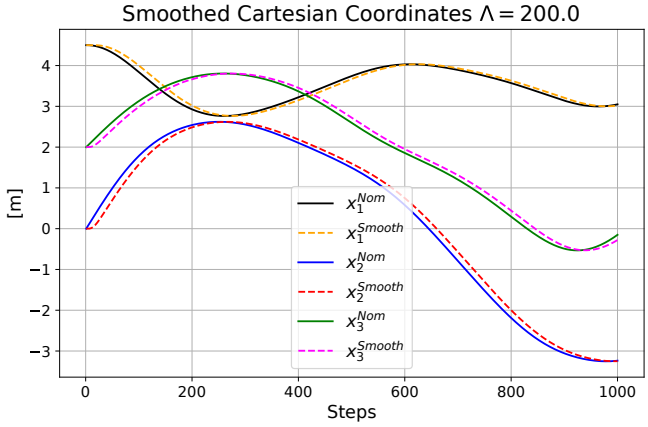

Fig. 8. The Cartesian coordinates of the trajectory of the TCP without constraint relaxation, with smoothing.

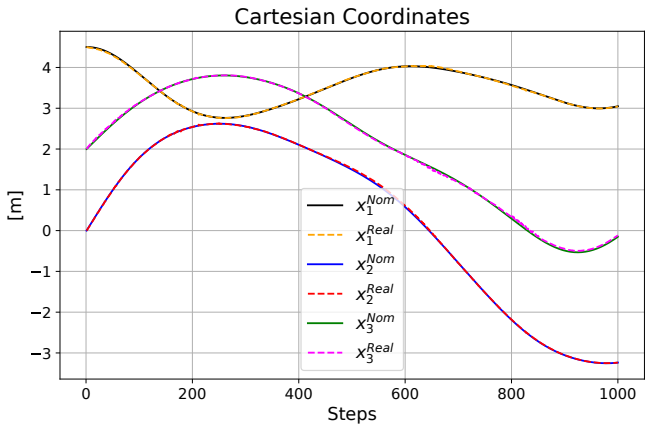

Fig. 9. The Cartesian coordinates of the trajectory of the TCP with constraint relaxation, without smoothing.

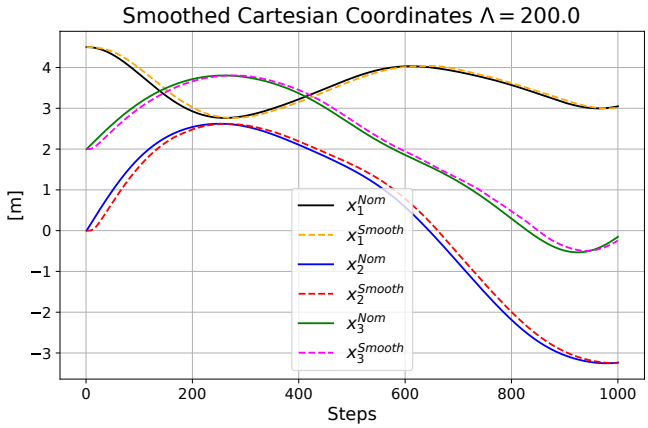

Fig. 10. The Cartesian coordinates of the trajectory of the TCP with constraint relaxation, with smoothing.

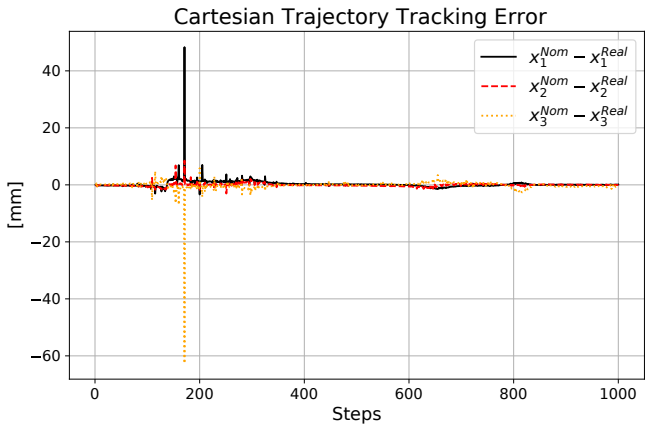

Fig. 11. The tracking error of the Cartesian coordinates of the trajectory of the TCP without constraint relaxation, without smoothing.

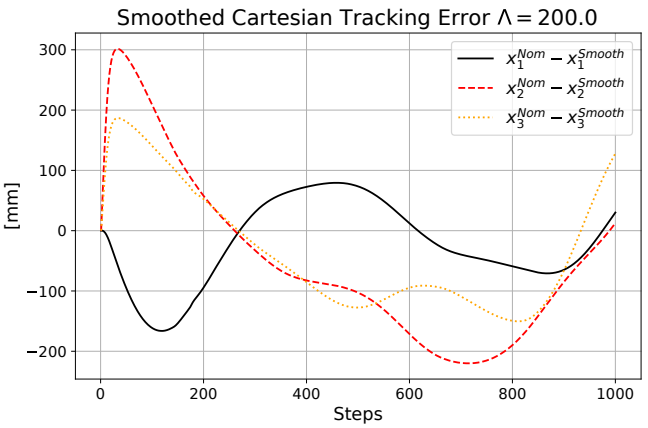

Fig. 12. The tracking error of the Cartesian coordinates of the trajectory of the TCP without constraint relaxation, with smoothing.

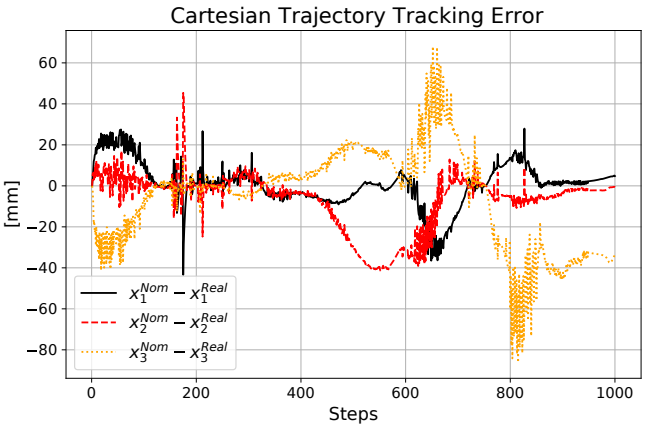

Fig. 13. The tracking error of the Cartesian coordinates of the trajectory of the TCP with constraint relaxation, without smoothing.

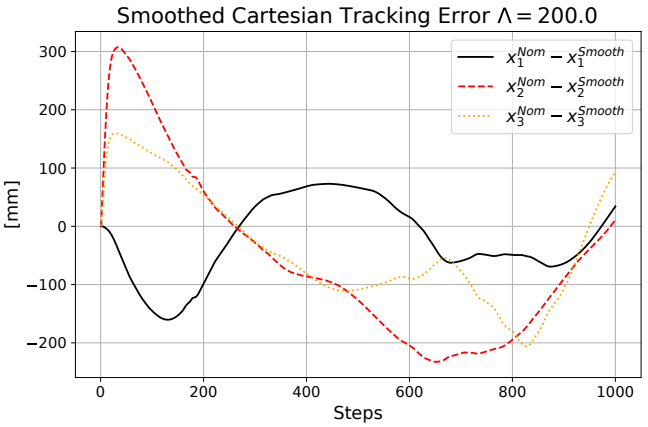

Fig. 14. The tracking error of the Cartesian coordinates of the trajectory of the TCP with constraint relaxation, with smoothing.

The hectic variation in the tracking error in Figs. 11, 12, 13, and 14 indicates that for obtaining a dynamically traceable

trajectory the smoothing phase is inevitable. Figs. 13, 14 also indicates the near singular sections where the tracking errors increased besides being very ”hectic”, and the constraint relaxation became visible.

Figs. 15,16, 17, 18 describe slight corrupting effect of smoothing on the orientation precision.

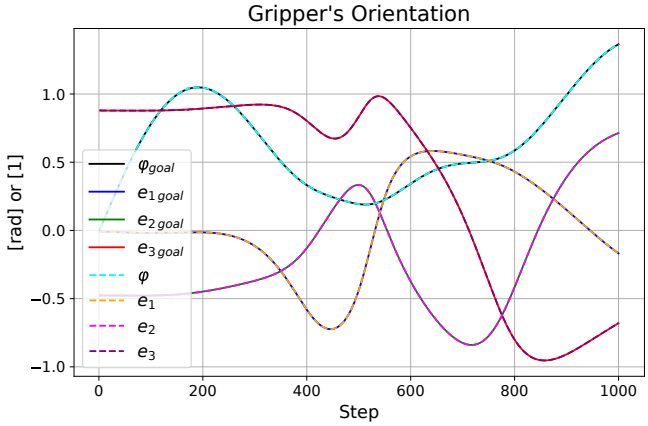

Fig. 15. The orientation of the TCP without constraint relaxation, without smoothing.

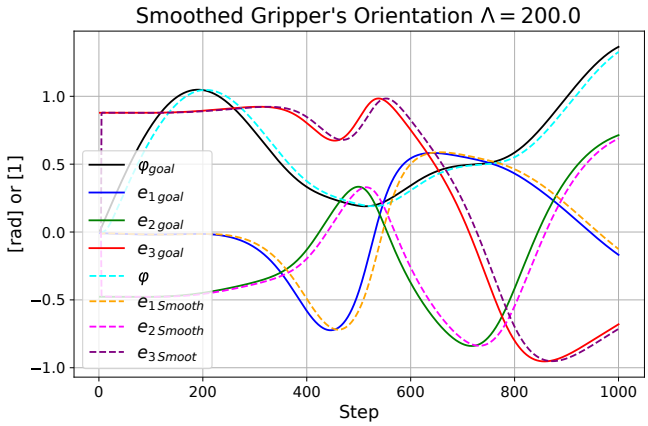

Fig. 16. The orientation of the TCP without constraint relaxation, with smoothing.

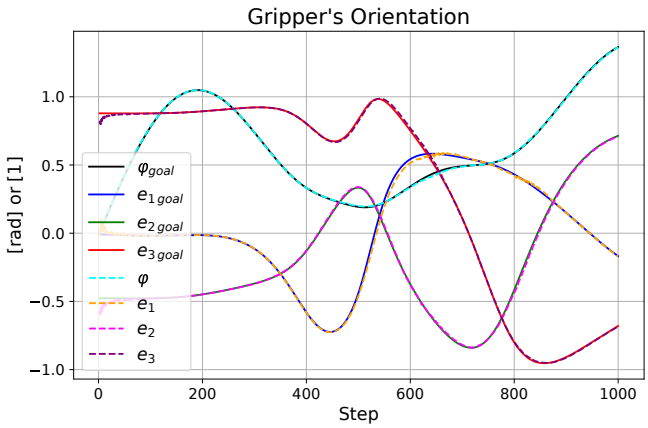

Fig. 17. The orientation of the TCP with constraint relaxation, without smoothing.

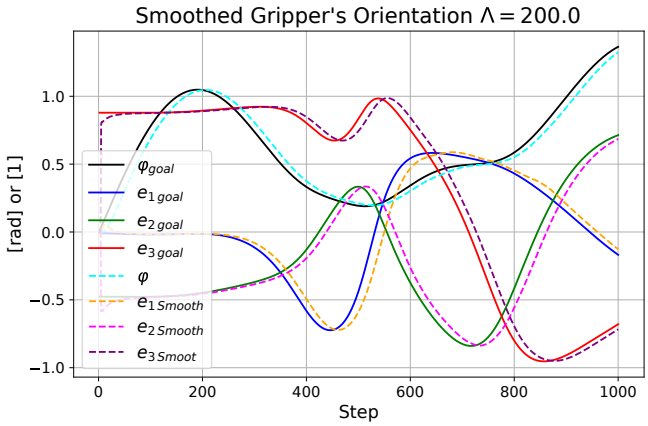

Fig. 18. The orientation of the TCP with constraint relaxation, with smoothing.

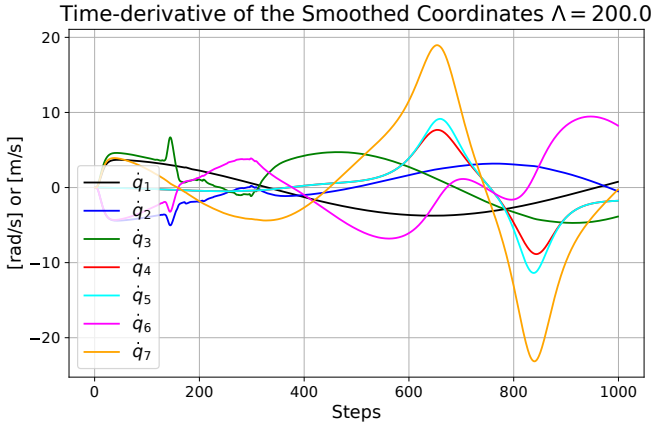

Fig. 19. The smoothed first time-derivatives of the joint coordinates: without constraint relaxation, with smoothing.

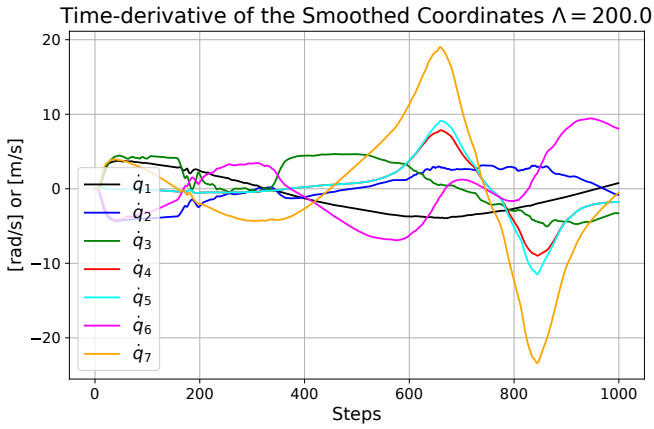

Fig. 20. The smoothed first time-derivatives of the joint coordinates with constraint relaxation, with smoothing.

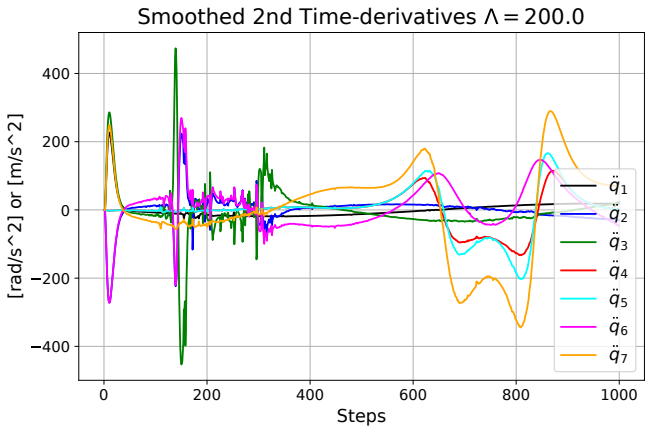

Fig. 21. The smoothed second time-derivatives of the joint coordinates p: without constraint relaxation, with smoothing.

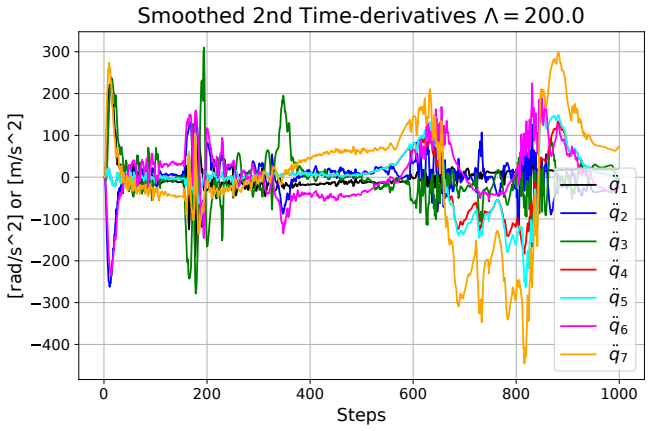

Fig. 22. The smoothed second time-derivatives of the joint coordinates with constraint relaxation, with smoothing.

Figs. 19, 20, 21, and 22 display that due to the filtering effect acceptable first and second time-derivatives were obtained for the joint coordinates. (It makes not sense to give the figures of the unfiltered quantities.)

In Figs. 23, 24, 25, 26, 27, 28, 29, and 30 the distribution of the rotations between the joint axles controlled by the constrained optimization can be observed.

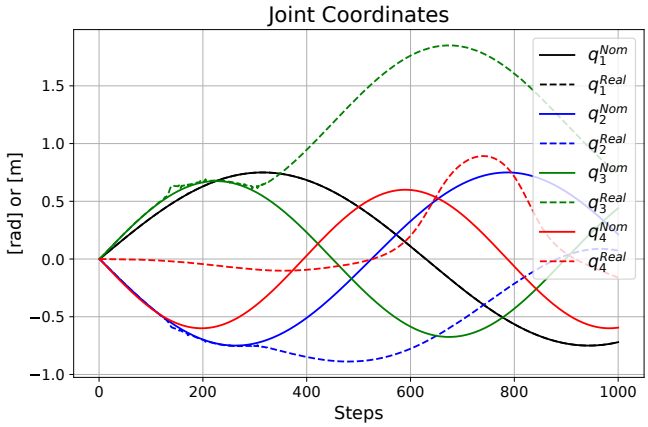

Fig. 23. The joint coordinates from 1 to 4 of the robot arm without constraint relaxation, without smoothing.

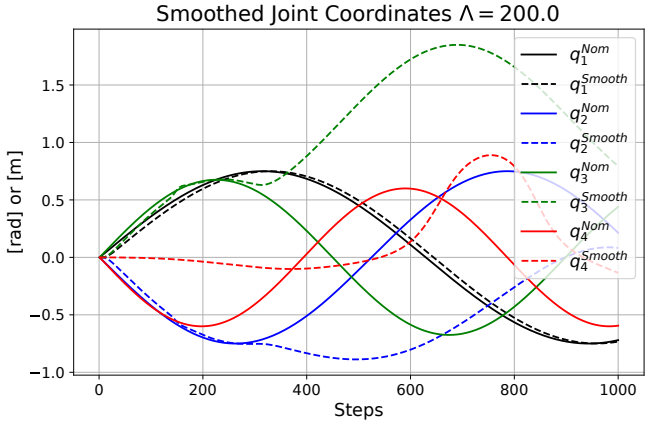

Fig. 24. The joint coordinates from 1 to 4 of the robot arm without constraint relaxation, with smoothing.

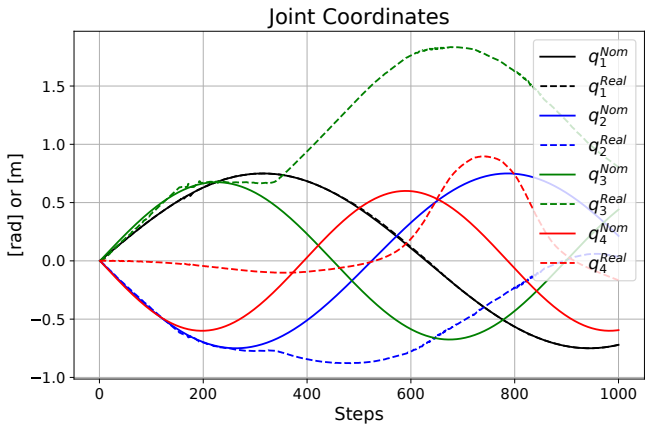

Fig. 25. The joint coordinates from 1 to 4 of the robot arm with constraint relaxation, without smoothing.

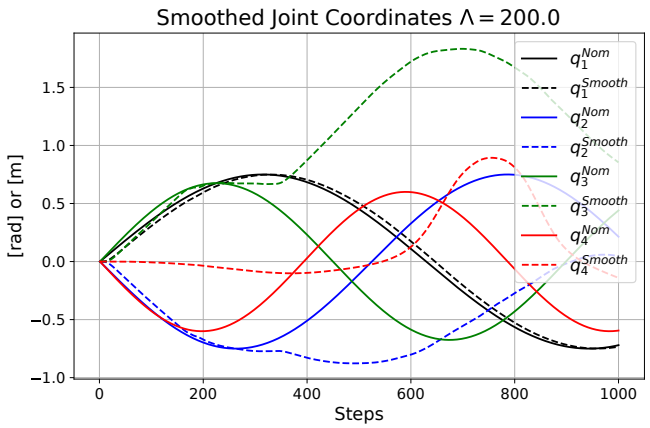

Fig. 26. The joint coordinates from 1 to 4 of the robot arm with constraint relaxation, with smoothing.

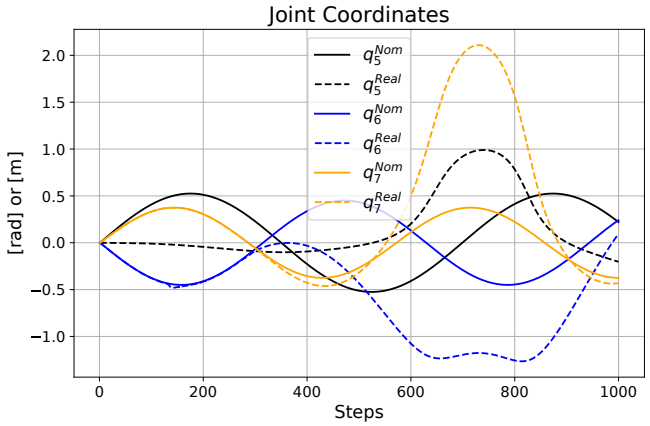

Fig. 27. The joint coordinates from 5 to 7 of the robot arm without constraint relaxation, without smoothing.

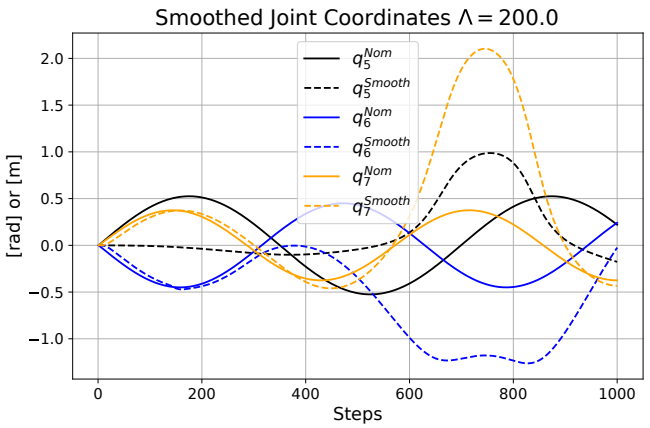

Fig. 28. The joint coordinates from 5 to 7 of the robot arm without constraint relaxation, with smoothing.

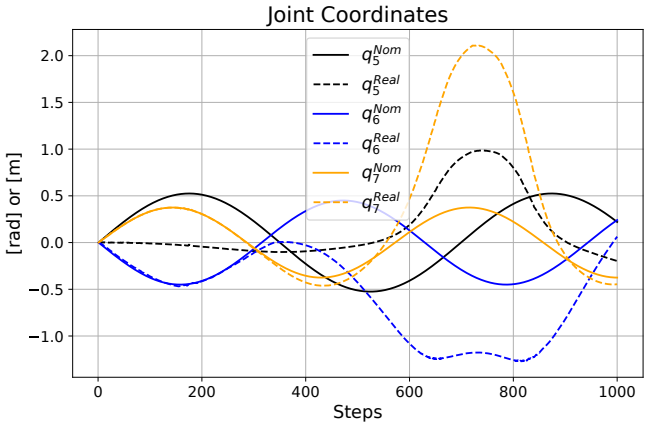

Fig. 29. The joint coordinates from 5 to 7 of the robot arm .

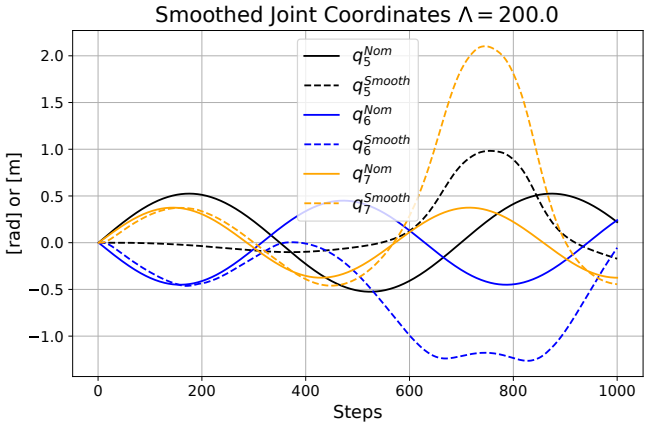

Fig. 30. The joint coordinates from 5 to 7 of the robot arm with constraint relaxation, with smoothing.

It is evident that due to the ambiguity caused by the redundancy huge differences can be observed between the *"nominal motion"* that was used for the generation of the trajectory and

the *"smoothed motion"* that was used for tracking the position and pose of the generated trajectory.

The effect of the *"width parameter of relaxation"*, i.e., w_S also deserves investigation.

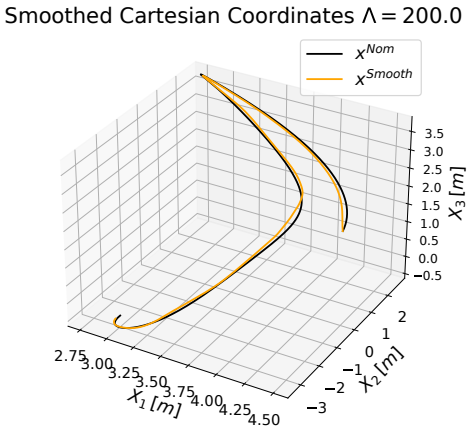

Fig. 31. The Cartesian figures of the trajectory of the TCP for $w_S = 1.5\,\mathrm{s}^{-1}$.

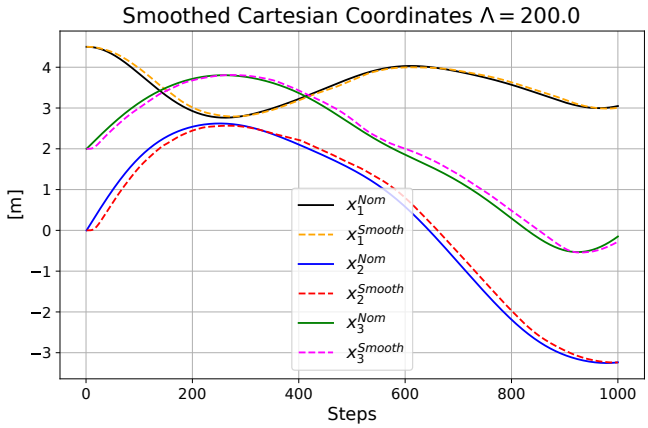

Fig. 32. The Cartesian figures of the trajectory of the TCP for $w_S = 1.5\,\mathrm{s}^{-1}$.

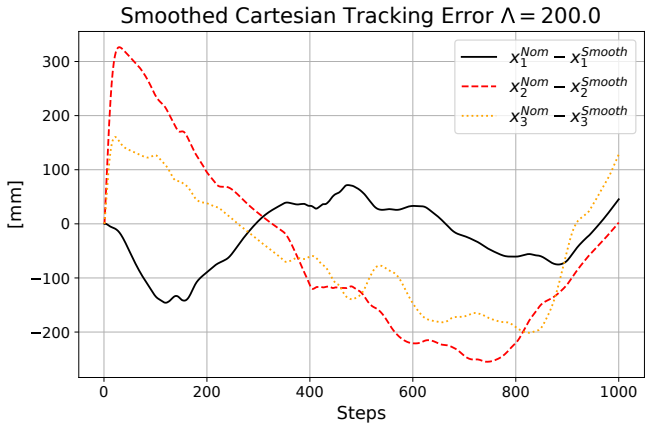

Fig. 33. The Cartesian tracking error for the location of the TCP for $w_S = 1.5\,\mathrm{s}^{-1}$.

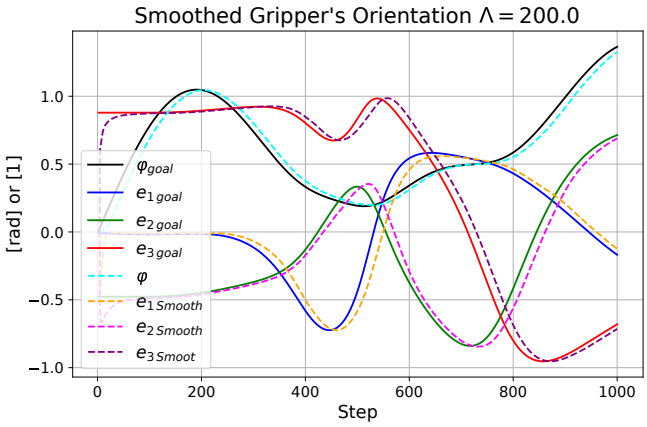

Fig. 34. The orientation tracking of the TCP for $w_S = 1.5\,\mathrm{s}^{-1}$.

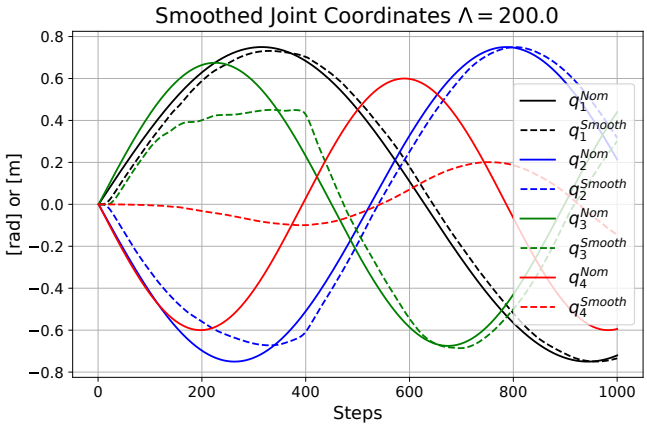

Fig. 35. The smoothed joint coordinates for $w_S = 1.5\,\mathrm{s}^{-1}$.

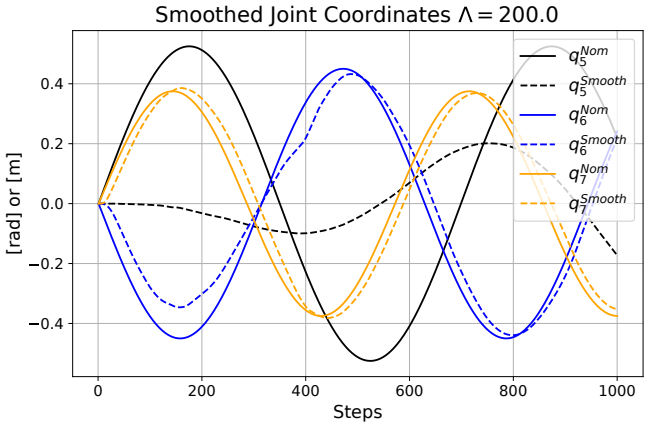

Fig. 36. The smoothed joint coordinates for $w_S = 1.5\,\mathrm{s}^{-1}$.

In the forthcoming figures w_S was decreased from $4.0\,\mathrm{s}^{-1}$ to $1.5\,\mathrm{s}^{-1}$. Only the "smoothed figures" are considered. It can be expected that this solution allows only smaller $\dot{q}_i$ first time-derivatives. Figs. 31, 32, 33, and 34 remained similar to their

previous counterparts. However, by suppressing the occurrence of higher $|\dot{q}_i|$ values the joint coordinates q_i were kept within a much more limited range than that of the previous examples.

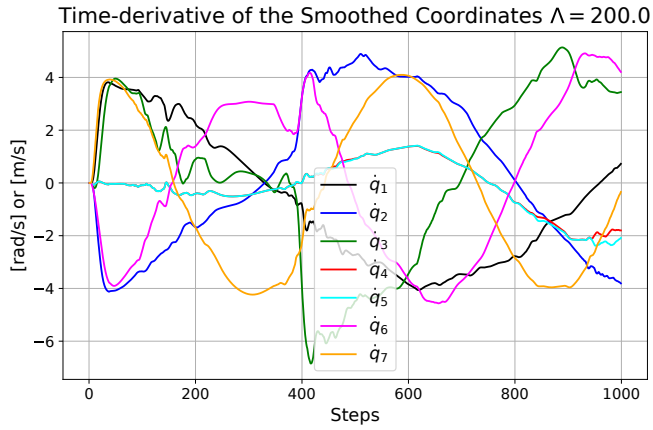

Fig. 37. The smoothed joint first time-derivatives of the joint coordinates for $w_S = 1.5\,\mathrm{s}^{-1}$.

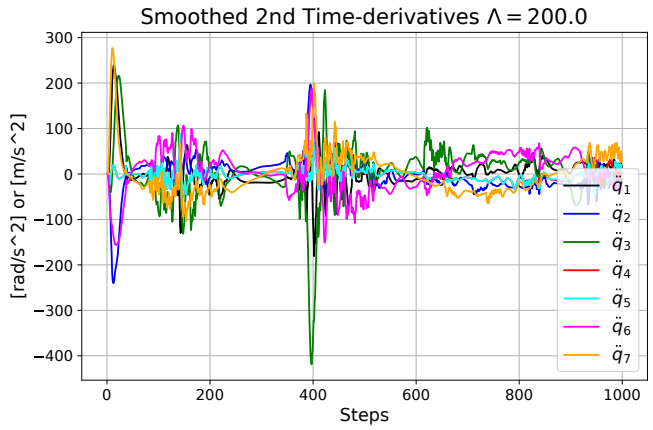

Fig. 38. The smoothed joint second time-derivatives of the joint coordinates for $w_S = 1.5\,\mathrm{s}^{-1}$.

The comparison of Figs. 19, 21 and 37 reveals that the new setting for $w_S = 1.5\,\mathrm{s}^{-1}$ kept the $|\dot{q}_i|$ values within a much narrower range than that of the setting $w_S = 4.0\,\mathrm{s}^{-1}$. The $|\ddot{q}_i|$ values remained within the same range.

IV. Conclusions

In this paper the solution of the differential inverse kinematic task of redundant open kinematic chains was investigated in the case of quite general (not necessarily quadratic) cost functions that allow the definition of far more sophisticated motion designs than the simple, Moore-Penrose pseudoinverse-based solutions. To evade the occurrence of impractically high first and second joint coordinate time-derivatives in the vicinity of the kinematic singularities a simple constraint relaxation strategy was applied. Furthermore, to accelerate the numerical process, instead introducing the usually great number of Lagrange multipliers as "co-state variables" only a single constraint term and a single Lagrange multiplier was applied that considerably reduces the complexity of the necessary numerical calculations. To compensate the not desirable effects of stopping the numerical algorithm at a given norm of the reduced gradient a simple third order trajectory smoothing strategy was applied, too. To exemplify the method a 7 degree of freedom, general structure open kinematic chain was considered that contained only rotary axles. For realizing the computations simple sequential code was developed with internal Euler integration by the use of Julia language. The computational results well testified that the applied method well utilizes the ample possibilities that are provided by the ambiguity of the solution of the redundant task.

References

[1] C.S.G. Lee and M. Ziegler. *RSD-TR-1-83 A geometric approach is solving the inverse kinematics of PUMA robots*. The University of Michigan, Ann Arbor, Michigan 48109-1109, 1983.

[2] A. Benitez, I. Huitzil, A. Casiano, J. De La Calleja, and M.A. Medina. Puma 560: Robot prototype with graphic simulation environment. *Advances in Mechanical Engineering*, 2(1):15–22, 2012.

[3] P. Chang. A closed-form solution for the control of manipulators with kinematic redundancy. In *Proceedings. 1986 IEEE International Conference on Robotics and Automation*, volume 3, pages 9–14. IEEE, 1986.

[4] J. Baillieul. Kinematic programming alternatives for redundant manipulators. In *Proceedings. 1985 IEEE International Conference on Robotics and Automation*, volume 2, pages 722–728. IEEE, 1985.

[5] O. Egeland. Task-space tracking with redundant manipulators. *IEEE Journal on Robotics & Automation*, 3(5):471–475, 1987.

[6] P. Chiacchio, S. Chiaverini, L. Sciavicco, and B. Siciliano. Closed-loop inverse kinematics schemes for constrained redundant manipulators with task space augmentation and task priority strategy. *International Journal of Robotics Research*, 10(4):410–425, 1991.

[7] N.D. Nenchev. Restricted jacobian matrices of redundant manipulators in constrained motion tasks. *The International journal of robotics research*, 11(6):584–597, 1992.

[8] E.H. Moore. On the reciprocal of the general algebraic matrix. *Bulletin of the American Mathematical Society*, 26(9):394–395, 1920.

[9] R. Penrose. A generalized inverse for matrices. *Proceedings of the Cambridge Philosophical Society*, 51:406–413, 1955.

[10] A. Ben-Israel and T.N.E. Greville. *Generalized Inverses*. Springer-Verlag, 2003.

[11] J.L. Lagrange, J.P.M. Binet, and J.G. Garnier. *Mécanique analytique (Analytical Mechanics) (Eds. J.P.M. Binet and J.G. Garnier)*. Ve Courcier, Paris, 1811.

[12] L.S. Lasdon, A.D. Waren, A. Jain, and M. Ratner. Design and testing of a generalized reduced gradient code for Nonlinear Programming. *ACM Transactions on Mathematical Software (TOMS)*, 4(1):34–50, 1978.

[13] J. Houston. Economic optimisation using Excel's Solver: A macroeconomic application and some comments regarding its limitations. *Computers in Higher Education Economics Review*, 11(1):2–5, 1997.

[14] D. Fylstra, L. Lasdon, J. Watson, and A. Waren. Design and use of the Microsoft EXCEL Solver. *Interfaces*, 28(5):29–55, 1998.

[15] E. Nævdal. Solving continuous-time optimal-control problem with a spreadsheet. *Journal of Economic Education*, 34(2):99–122, 2003.

[16] J.I. Silva and A. Xabadia. Teaching the two-period consumer choice model with EXCEL-SOLVER. *Australasian Journal of Economics Education*, 10(2):24–38, 2013.

[17] A. Ionescu. Microsoft Office Excel 2010 operational research in Excel 2010. *International Journal of Computer and Information Technology*, 02(05):1026–1064, 2013.

[18] H. Karabulut. Physical meaning of Lagrange multipliers. *European Journal of Physics (physics.ed-ph); General Physics (physics.gen-ph)*, 27:709–718, 2007.

[19] H.B. Callen. *Thermodynamics and an Introduction to Thermostatistics (Second Edition)*. John Wiley & Sons, New York, Chichester, Brisbane, Toronto, Singapore, 1960.

[20] W.R. Hamilton. On a general method in dynamics. *Philosophical Transactions of the Royal Society, part II for 1834*, pages 247–308, 1834.

[21] W.R. Hamilton. Second essay on a general method in dynamics. *Philosophical Transactions of the Royal Society, part I for 1835*, pages 95–144, 1835.

[22] R.E. Kalman. Contribution to the theory of optimal control. *Boletin Sociedad Matematica Mexicana*, 5(1):102–119, 1960.

[23] B.D.O. Anderson and J.B. Moore. *Optimal Control: Linear Quadratic Methods*. Prentice – Hall International, Inc., A Division of Simon & Schuster, Englewood Cliffs, NJ 07632, 1989.

[24] T. Çimen. State-dependent Riccati equation in nonlinear optimal control synthesis. *In the Proc. of the Special International Conference on Complex Systems: Synergy of Control, Communications and Computing - COSY 2011, Hotel Metropol Resort, Ohrid, Republic of Macedonia, September, 16 – 20, 2011*, pages 321–332, 2011.

[25] K. Levenberg. A method for the solution of certain non-linear problems in least squares. *Quarterly of Applied Mathematics*, 2:164–168, 1944.

[26] D. Marquardt. An algorithm for least-squares estimation of nonlinear parameters. *J. Soc. Indust. Appl. Math.*, 11(2):431–441, 1963.

[27] H. Issa, B. Varga, and J.K. Tar. Accelerated reduced gradient algorithm for solving the inverse kinematic task of redundant open kinematic chains. *In proc. of the IEEE 15th International Symposium on Applied Computational Intelligence and Informatics (SACI 2021), May 19-21, 2021 in Timisoara, Romania.*, pages 387–392, 2021.

[28] H. Issa, B. Varga, and J.K. Tar. A receding horizon-type solution of the inverse kinematic task of redundant robots. *In proc. of the IEEE 15th International Symposium on Applied Computational Intelligence and Informatics (SACI 2021), May 19-21, 2021 in Timisoara, Romania.*, pages 231–236, 2021.

[29] J. Richalet, A. Rault, J.L. Testud, and J. Papon. Model predictive heuristic control: Applications to industrial processes. *Automatica*, 14(5):413–428, 1978.

[30] Zs. Horváth and A. Edelmayer. Solving the modified filter algebraic Riccati equation for H-infinity fault detection filtering. *Acta Universitatis Sapientiae, Electrical and Mechanical Engineering*, 9:57–77, 2017.

[31] O. Rodrigues. Des lois géometriques qui regissent les déplacements d' un systéme solide dans l' espace, et de la variation des coordonnées provenant de ces déplacement considérées indépendent des causes qui peuvent les produire (Geometric laws which govern the displacements of a solid system in space: and the variation of the coordinates coming from these displacements considered independently of the causes which can produce them). *J. Math. Pures Appl.*, 5:380–440, 1840.

[32] J. Bezanson, A. Edelman, S. Karpinski, and V.B. Shah. Julia. *https://julialang.org*, Last time visited: 5 May 2019.

[33] B. Lantos and Zs. Bodó. High level kinematic and low level nonlinear dynamic control of unmanned ground vehicles. *Acta Polytechnica Hungarica*, 16(1):97–117, 2019.